Contrib Mineral Petrol (2008) 156:273–288
DOI 10.1007/s00410-008-0284-2

ORIGINAL PAPER

The geochemistry of mantle chromitites from the northern part of the Oman ophiolite: inferred parental melt compositions

Hugh Rollinson

Received: 7 October 2007 / Accepted: 4 February 2008 / Published online: 21 February 2008

Abstract Chromitites from a single section through the mantle in the Oman ophiolite are of two different types. Low-cr# chromitites, of MORB affinity are found in the upper part of the section, close to the Moho. High-cr# chromitites, with arc affinities are found deeper in the mantle. Experimental data are used to recover the compositions of the melts parental to the chromitites and show that the low-cr# chromitites were derived from melts with 14.5–15.4 wt% Al_2O_3, with 0.4 to 0.9 wt% TiO_2 and with a maximum possible mg# of 0.76. In contrast the high-cr# chromitites were derived from melts with 11.8–12.9 wt% Al_2O_3, 0.2–0.35 wt% TiO_2 and a maximum melt mg# of 0.785. Comparison with the published compositions of lavas from the Oman ophiolite shows that the low-cr# chromitites may be genetically related to the upper (Lasail, and Alley) pillow lava units and the high-cr# chromitites the boninites of the upper pillow lava Alley Unit. The calculated TiO_2–Al_2O_3 compositions of the parental chromitite magmas indicate that the high-cr# chromitites were derived from high-Ca boninitic melts, produced by melting of depleted mantle peridotite. The low-cr# chromitites were derived from melts which were a mixture of two end-members—one represented by a depleted mantle melt and the other represented by MORB. This mixing probably took place as a result of melt–rock reaction.

Electronic supplementary material The online version of this article (doi:10.1007/s00410-008-0284-2) contains supplementary material, which is available to authorized users.

Communicated by C. Ballhaus

H. Rollinson (✉)
Department of Earth Sciences, Sultan Qaboos University,
Box 36, Postal Code 123, Al-Khodh, Muscat,
Sultanate of Oman
e-mail: hrollin@squ.edu.om

Keywords Mantle · Chromite · Harzburgite · Boninite · Oman ophiolite

Introduction

Ever since the seminal papers of Irvine (published in 1965, 1967), the mineral chromite has been used to determine the petrogenetic conditions of evolving mafic magmas. More recently it has also been recognized that chromites formed in mafic melts in different tectonic environments have compositional differences and so chromite has also become a powerful indicator of the former tectonic setting of mafic and ultramafic rocks (Kamenetsky et al. 2001). In particular, chromite compositions have been used as a means of identifying the former tectonic setting of fragments of the mantle now found in ophiolite sequences (see, for example, Zhou and Robinson 1997).

In this study chromitites are described from a single transect through the mantle sequence of the northern part of the Oman ophiolite in Wadi Rajmi (Fig. 1). They are significant because they show important compositional differences which appear to be correlated with depth beneath the Moho. These differences are most clearly seen in the Cr/Cr + Al ratio of the chromites (the cr#), and elsewhere in the Oman ophiolite have been interpreted as indicating different tectonic settings for the formation of the chromitites (Ahmed and Arai 2002).

Chromitite pods, hosted in depleted mantle harzburgite, from the shallow part of the mantle section in Wadi Rajmi, northern Oman, contain chromites with cr# between 0.52 and 0.64. These would typically be interpreted as chromites in equilibrium with a MORB melt indicating that the enclosing mantle harzburgites formed in a sub-ocean-ridge environment (Fig. 2a). These low-cr#

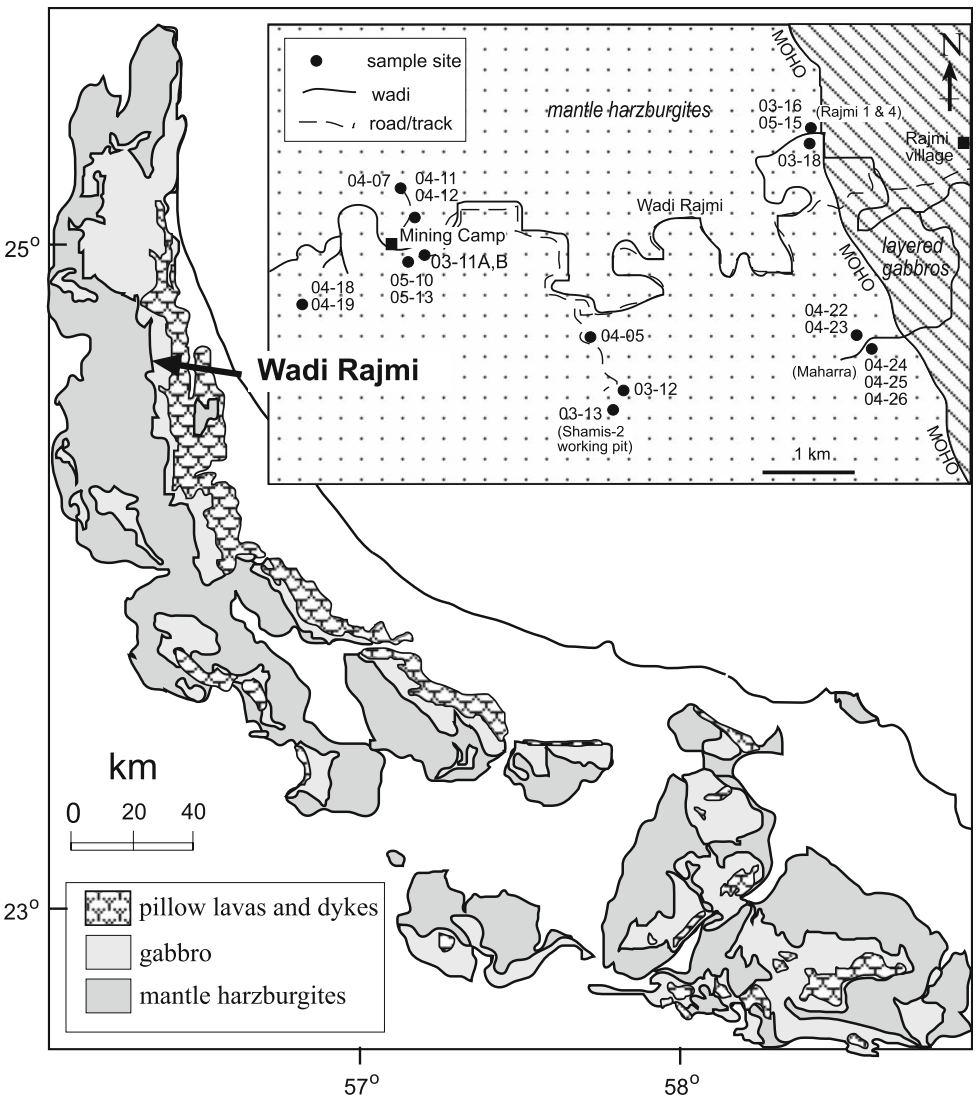

Fig. 1 Map of the Oman ophiolite showing the location of the study area. The *inset* map shows the sample locations in Wadi Rajmi

samples have higher Al_2O_3 and a wide range of TiO_2 concentrations consistent with the field of MORB spinels identified by Kamenetsky et al. (2001) (Fig. 2b). In contrast chromitites from deeper in the same mantle section have cr# between 0.71 and 0.77, values which are much closer to chromites formed in equilibrium with boninitic melts (Fig. 2a) and which would appear to indicate their genesis in a supra-subduction zone environment. These chromites have lower Al_2O_3 and low TiO_2 concentrations consistent with the field of arc spinels of Kamenetsky et al. (2001) (see Fig. 2b).

It has been proposed by Edwards et al. (2000) that high-Cr concentrations in the mantle, indicated by the presence of abundant chromitite pods, represent regions of particularly high melt flux through the mantle. Hence, in this study it is assumed that the chromite in chromitite pods within the harzburgitic mantle has formed by fractional crystallisation from mafic melts percolating through the depleted

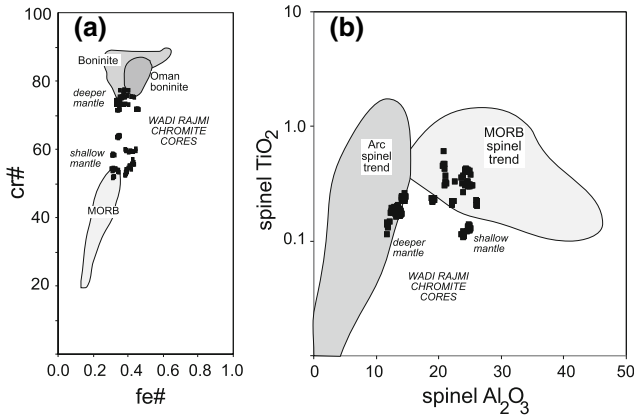

Fig. 2 **a** Cr# vs fe# of core compositions for Wadi Rajmi chromites plotted relative to the fields of boninites, the Oman boninites and MORB (see Rollinson 2005) for data sources for the boninite and MORB fields). **b** Al_2O_3 and TiO_2 data for the core compositions for Wadi Rajmi chromites from deep and shallow mantle, plotted relative to the fields of arc and MORB spinels (after Kamenetsky et al. 2001)

mantle harzburgite. It will be argued that the mineral chemistry of the chromite and of the associated interstitial silicate minerals, and the order in which these minerals crystallized, preserve a memory of the composition of the parental melt. This view is supported by experimental studies which show that the principal control on chromite mineral chemistry is the composition of the melt from which it crystallizes (see references in Kamenetsky et al. 2001).

This study therefore has two main goals. The first is to utilize the chemistry of the Wadi Rajmi mantle chromitites and the associated silicates in order to calculate the composition(s) of their parental melts and thus characterize the nature of melts which are generated within and migrate through depleted mantle. In addition changes in mineral chemistry recorded by mineral zoning can be used to track subtle changes in melt composition during chromitite crystallisation. Secondly, this history of melt migration through already depleted mantle provides further insight into the history of melt extraction in a segment of ophiolitic mantle.

Previous geochemical studies on the mantle section of the Oman ophiolite

The mantle section of the Oman ophiolite preserves perhaps the largest area of mantle harzburgite on Earth. About 10,000 km^2 are currently exposed. Recent geochemical studies show that the harzburgites have suffered extensive melt extraction and are highly depleted in incompatible elements. Monnier et al. (2006) state that there has been on average 16% melt extraction, and Le Mée et al. (2004) and Monnier et al. (2006) estimate that the range was between 10 and 30%. In fact Le Mée et al. (2004) argue that it is possible to identify zones of greater and lesser melt extraction along the 420 km length of the ophiolite suggesting a strong similarity with the segmentation observed in modern mid-ocean ridges. Although the refractory nature of the Oman mantle harzburgites is its dominant geochemical feature, Godard et al. (2000) showed that there are regions where harzburgite has been *re*-fertilized, through the later addition of light rare earth-enriched melts. Melt migration though the Oman harzburgites has also been discussed by Braun and Kelemen (2002) who argue that the centimetre-to-decimetre-wide dunitic zones are former high-porosity melt channels created by a dissolution instability.

Early studies on chromitites in the mantle section of the Oman ophiolite focused on their structural relations to the enclosing harzburgites (see for example Ceuleneer and Nicolas 1985; Nicolas and Al-Azri 1991). A particular focus was the Maqsad area, in the southern part of the ophiolite, where a large number of chromitite bodies are clustered close to the Moho. Lorand and Ceulneer (1989) drew attention to the presence of hydrous silicate inclusions in the chromite; Leblanc and Ceuleneer (1992) described the pattern of magmatic flow in a chromitite dyke and Schiano et al. (1997) calculated the composition of the parental magma from melt inclusions.

Auge (1987), working in the north of Oman, was the first to recognize the wide range of chromite compositions and their variation with depth within the Oman ophiolite, which he explained in terms of more and less aluminous parental melts. More recently Ahmed and Arai (2002) demonstrated the compositional difference between early, concordant chromitite pods (cr# = 0.62 and PGE-poor) and a later, discordant dyke (cr# = 0.71, PGE-rich) in Wadi Hilti, northern Oman. The two localities are about 200 m apart. Ahmed and Arai (2002) interpreted these two different types of chromite as the product of two discrete mantle melting events, the first beneath a fast-spreading ocean ridge and the later one in a supra-subduction zone environment. In contrast, in a review of the Oman chromitite dataset, Rollinson (2005) drew attention to the continuum of compositions between low-cr# and high-cr# chromites and suggested that this reflected evolving melt compositions produced through melt–rock reaction within the mantle, but which did not require a change in tectonic environment.

Study area and field relationships

The samples in this study are from chromitite pods located in harzburgites from the mantle section of the Oman ophiolite. They were collected from a single transect through the ophiolite in Wadi Rajmi in the northern part of Oman and represent chromitites formed at different depths beneath the Moho (Fig. 1). Wadi Rajmi was selected for this study because of the abundance of chromitite pods in this part of the mantle section. It was noted earlier that a high frequency of chromitite pods might represent a region of particularly high melt flux through the mantle (Edwards et al. 2000), although the Wadi Rajmi area projects onto 'discontinuity D3' in the studies of Le Mée et al. (2004) and Monnier et al. (2006), representing a region of particularly low-melt extraction. This apparent discrepancy is unresolved. A summary of the field relationships and petrography at each locality, ordered by increasing depth beneath the Moho is given as electronic supplementary material Table 1. Changes in mineral chemistry are summarized in Table 1 and Fig. 3. Although the localities are defined in terms of their distance from the Moho, the dip of this section is on average 30° west, and so true depths are about half of those shown.

Table 1 Summary of mineral compositions from the Wadi Rajmi chromitites

	Sample	Horizontal distance to Moho (meters)	Chromite cr# (core max)	Chromite cr# (core min)	Chromite fe# (core max)	Chromite fe# (core min)	Chromite TiO_2 (max)	Chromite TiO_2 (min)	Olivine mg# core (max)	Olivine mg# core (min)	Olivine NiO	Cpx mg# (max)	Cpx mg# (min)	Opx mg#	Amph mg # (max)	Amph mg # (min)
	Chromitites															
Rajmi	05–15	100	0.598	0.595	0.391	0.384	0.371	0.305				0.968	0.957		0.957	0.937
	03–16	130	0.601	0.594	0.443	0.411	0.600	0.470				0.953	0.947		0.941	0.930
	03–18	200	0.569	0.523	0.427	0.382	0.460	0.304							0.932	0.918
Maharra	04–24	492	0.519	0.516	0.309	0.330	0.226	0.215				0.948	0.931	0.926		
	04–25	494	0.537	0.537	0.339	0.342	0.329	0.326	0.944	0.944	0.480				0.950	0.947
	04–26	496	0.538	0.532	0.348	0.342	0.310	0.296	0.944	0.944	0.490				0.930	0.927
	04–23	547	0.543	0.527	0.330	0.304	0.136	0.123				0.938	0.936		0.975	0.971
	04–22	550	0.540	0.535	0.323	0.312	0.142	0.121				0.937	0.937	0.931	0.989	0.974
Shamis	04–05	3,500	0.585	0.581	0.310	0.314	0.220	0.230	0.948	0.948	0.550					
	03–12	3,600	0.639	0.632	0.249	0.242	0.235	0.217	0.946	0.946	0.535					
Mining Camp	04–07	4,960	0.773	0.767	0.402	0.377	0.150	0.140							0.986	0.967
	04–11	5,050	0.734	0.730	0.412	0.326	0.180	0.160	0.958	0.955	0.640					
	03–11a	5,120	0.754	0.751	0.375	0.353	0.196	0.175	0.958	0.955	0.585					
	03–11b	5,120	0.754	0.751	0.378	0.350	0.192	0.185	0.951	0.949	0.549				0.968	0.968
	05–13	5,365	0.742	0.740	0.338	0.328	0.185	0.168	0.958	0.959	0.720					
	05–10	5,370	0.748	0.736	0.366	0.347	0.180	0.190	0.959	0.959	0.830					
Deepest	04–18ct	6,500	0.714	0.713	0.345	0.336	0.239	0.223	0.958	0.958	0.740					
	04–19ct	6,510	0.717	0.714	0.447	0.443	0.242	0.236								
	Dunites															
Shamis	03–13	3,400	0.561	0.554	0.182	0.159	0.130	0.112	0.916	0.916	0.429	0.949	0.940	0.917	0.946	0.945
Deepest	04–18du	6,500	0.717	0.716	0.355	0.345	0.241	0.241	0.953	0.953	0.610					
	04–19du	6,510	0.718	0.714	0.481	0.438	0.233	0.204	0.923	0.923	0.460	0.954	0.950			

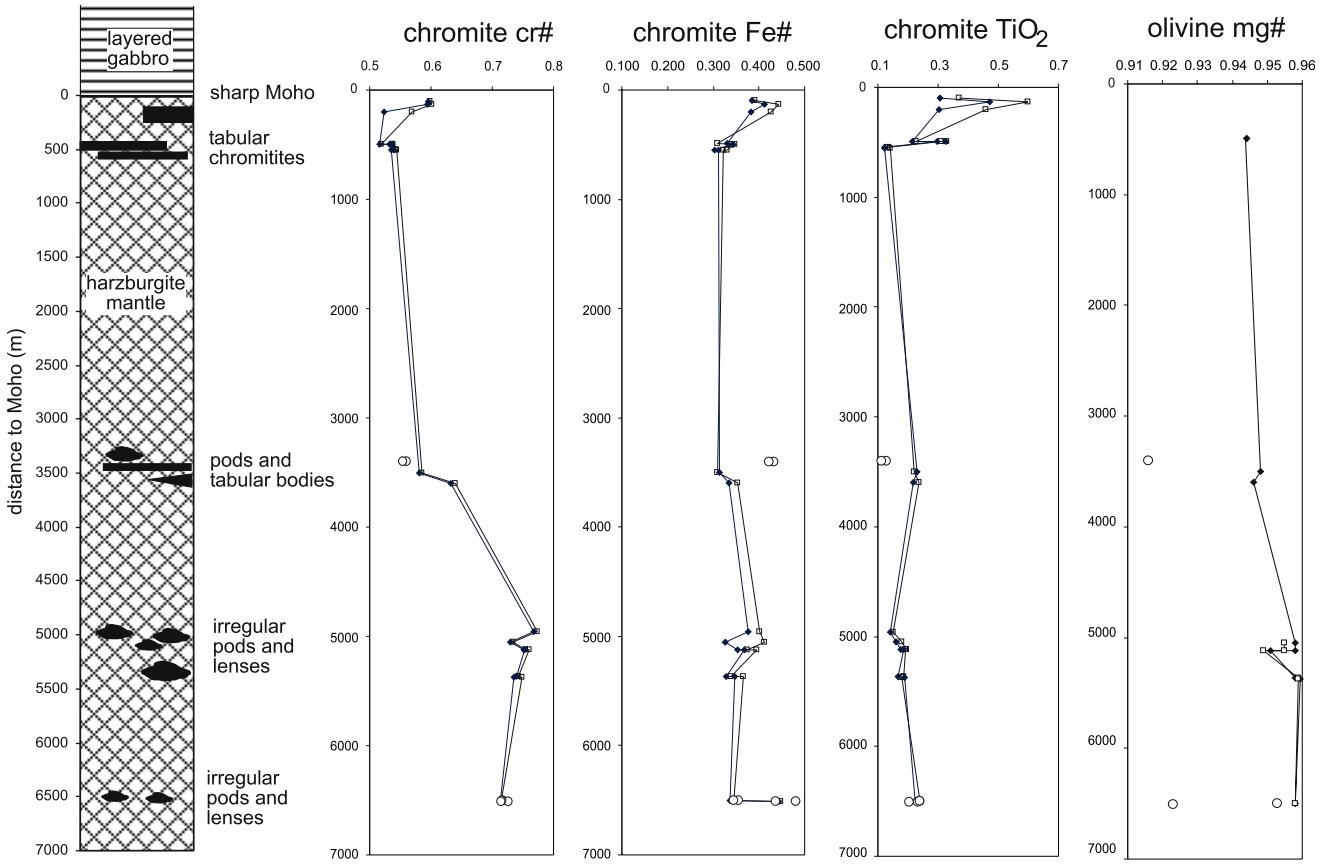

Fig. 3 A stratigraphic section for the Wadi Rajmi mantle section of the Oman ophiolite showing the position of the different chromitite bodies and the compositional change in chromite cr#, fe# and TiO_2 and olivine mg# with depth below the Moho. Maximum and minimum compositions shown as *open squares* and *filled diamonds*, respectively. *Circles* are for dunitic compositions. Data in Table 1

Analytical methods

Mineral analyses were made on a Cameca SX100 electron probe microanalyser at the Department of Earth Sciences, University of Bristol, using wavelength dispersive detectors and the ZAF data reduction procedure. Operating conditions were 20 kV accelerating voltage, 20 nA beam current; the beam diameter was ca. 1 μm. The standards used were olivine (Mg, Si), albite (Al), wollastonite (Ca), ilmenite (Fe, Ti), chromite (Cr), and V, Mn, Ni and Zn metal.

This study is based upon more than 900 chromite analyses, more than 220 olivine analyses and more than 200 analyses of associated minor phases on 19 samples from 10 localities within Wadi Rajmi. Multiple analyses were performed on single grains, usually as a traverse across the grain in order to detect zoning. Fe(III) in chromite was calculated using the charge balance equation of Droop (1987) and by re-calculating analyses to 24 cations.

Mineral chemistry

Chromite

The full range of recorded chromite compositions from both cores and rims is very broad—from fe# 0.225–0.634, cr# 0.355–0.937, much greater than that recorded for core compositions alone (fe# 0.304–0.462, cr# 0.514–0.773)—see Fig. 4 and Table 2. There are two reasons for the spread in fe# in chromite rim compositions. Firstly, many chromite grains are zoned and have Fe-rich rims. This is believed to be because of Fe–Mg exchange with olivine during the slow cooling of the mantle. This is discussed more fully later. Secondly, some grains have experienced late grain boundary oxidation and Fe-enrichment. These oxidized grains also contain higher levels of Fe(III) replacing Al and so have an elevated Cr/Cr + Al ratio (cr#). Grains with an abnormally low cr# tend to be associated with sulphide grains (FeNiS-NiS intergrowths) located at chromite grain boundaries. These areas of

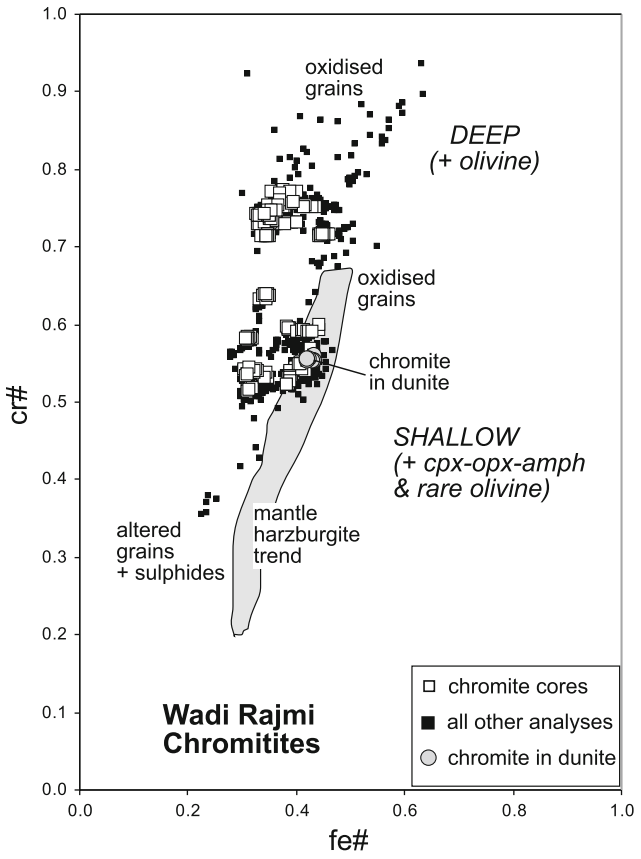

Fig. 4 Chromite compositions for the Wadi Rajmi chromites plotted on a fe#–cr# diagram. Core compositions: *open squares*, rim compositions: *filled squares*. Chromite in dunite: *grey circles*. The diagram shows the difference in composition between the chromitites emplaced in the deep and shallow mantle and identifies grains which have oxidized rims and those which have experienced alteration adjacent to sulphide grains. The mantle harzburgite trend, shown in *grey*, is from Le Mée et al. (2004)

chromite alteration have unusually high Al and Mg—hence low Cr/Cr + Al ratios. These features are also apparent on a trivalent ion (Al–Fe(III)–Cr) ternary diagram (Fig. 5a). More subtle is the higher concentration of Fe(III), as estimated from mineral stoichiometry, in the shallow mantle chromites relative to those in the deeper mantle. In addition the Fe(III) content of chromite hosted in dunite is higher than that in the associated chromitites (Fig. 5b).

Chromite cores also show significant variation in both cr# and Ti. These features are believed to be primary, for the rates of diffusion of Cr, Al and Ti in chromite are slow, even at mantle temperatures. The differences in cr# and Ti will form the basis for much of the future discussion in this study.

The minor element Mn correlates positively with Fe and Ni with Mg. There is a narrow spread of Ti values in the high-cr# chromites (0.15–0.24 wt% TiO_2) and a broader spread of values in chromites with a lower cr# (0.14–0.60 wt% TiO_2). V concentrations are higher in the low-cr# chromites and lower in the high-cr# chromites. Chromite in the dunite at Shamis has a higher Zn content (average 0.21 wt% ZnO) relative to chromite in chromitites (average 0.05 wt% ZnO).

Olivine

Olivine is more commonly associated with the deeper, higher-cr# chromites and is absent from several of the shallow chromitite bodies. Olivine core compositions in chromitites vary in composition from $Fo_{94.4}$ to $Fo_{95.9}$ and in dunites from $Fo_{91.2}$ to $Fo_{95.3}$ (electronic supplementary material Table 2). Many olivine grains are zoned with Mg-rich rims and Fe-rich cores. The NiO content of olivine varies from 0.48 to 0.89 wt% in the chromitites and increases with depth; it varies from 0.39 to 0.61 wt% in the dunites. There is a positive correlation between Ni in olivine and Fo-content, although the Ni content of olivine in the dunites is lower than olivine in the chromitites, and the two data groups define different slopes on a Mg–Ni plot. This difference is probably a consequence of the differing degrees of subsolidus exchange of Mg and Ni between olivine and chromite in the chromitites and dunites. There is also a positive correlation between Mn in olivine and Fe-content.

The results of Fe–Mg exchange thermometry between olivine and chromite using the Ballhaus et al. (1991) olivine-spinel thermometer give temperatures in the range 550–700°C (rims) and 640–800°C (cores). Coexisting but isolated olivine-spinel cores from a dunite-chromitite pair give temperatures in the range 921–959°C. All these temperatures are substantially below mantle temperatures and indicate significant Fe–Mg equilibration during cooling. This accounts for the Mg-rich rims in olivine grains and the Fe-rich rims to chromites. Small olivine grains in chromitites do not therefore preserve their original composition, even in the cores of grains. However, on mass balance grounds the Fe–Mg ratios of olivines in dunites and chromites in chromitites are more likely to be original.

Clinopyroxene

Clinopyroxene is found as a minor interstitial phase in the shallow (low-cr#) chromitites and is also a minor component of dunites. Clinopyroxene in the chromitites varies in Al-content from 1.0 to 2.8 wt% Al_2O_3 and in the dunites from 1.8 to 2.6 wt% Al_2O_3 (electronic supplementary material Table 2). The Cr-content varies from 0.31 to 1.42 wt% in the chromitites and from 0.09 to 0.11 wt% in the dunites. On cation plots there are inverse correlations between Si and Al, Si and Cr and Cr + Al and Ca, indicating a Tschermaks substitution.

Table 2 Initial chromite compositions used as indicators of melt compositions

Locality	Deep chromitites				Shallow chromitites					
	Mining camp			Deepest	Shamis	Shamis	Rajmi	Maharra	Maharra	Rajmi
	High Cr	Large pit	Small pit			Small	North	North	South	South
Rock	04–07	05–13	04–11	04–18	03–12	04–05	05–15	04–22	04–25	03–18
SiO_2	0.046	0.000	0.009	0.000	0.000	0.000	0.041	0.000	0.002	0.013
TiO_2	0.140	0.168	0.181	0.223	0.237	0.222	0.305	0.120	0.329	0.422
Al_2O_3	11.721	13.280	13.907	14.472	19.134	22.421	20.998	24.548	24.510	24.397
MgO	12.835	13.914	14.311	13.844	16.793	15.173	13.349	15.046	14.534	13.474
FeO	14.401	14.521	15.669	15.228	14.104	15.634	17.964	15.059	16.506	19.365
MnO	0.181	0.181	0.183	0.160	0.186	0.175	0.222	0.166	0.191	0.228
CaO	0.003	0.004	0.001	0.007	0.012	0.006	0.000	0.009	0.000	0.000
NiO	0.145	0.108	0.142	0.123	0.151	0.168	0.136	0.161	0.140	0.143
ZnO	0.025	0.033	0.032	0.042	0.056	0.053	0.039	0.051	0.034	0.077
Cr_2O_3	59.563	56.469	55.700	53.907	50.109	46.426	46.495	43.715	42.354	41.701
V_2O_3	0.147	0.152	0.163	0.178	0.172	0.225	0.127	0.150	0.210	0.187
Total	99.21	98.83	100.30	98.18	100.95	100.50	99.68	99.03	98.81	100.01
Recalculated to 24.0 cations										
Si	0.012	0.000	0.002	0.000	0.000	0.000	0.010	0.000	0.000	0.003
Ti	0.027	0.032	0.034	0.043	0.044	0.040	0.057	0.022	0.060	0.077
Al	3.582	4.012	4.126	4.376	5.534	6.381	6.119	7.016	7.042	6.988
Fe2	3.002	2.646	2.592	2.677	2.802	2.498	3.065	2.505	2.705	3.109
Fe3	0.120	0.467	0.706	0.590	0.645	0.659	0.649	0.549	0.659	0.826
Mn	0.040	0.039	0.039	0.035	0.039	0.036	0.046	0.034	0.039	0.047
Mg	4.961	5.318	5.370	5.296	5.160	5.463	4.921	5.440	5.282	4.882
Ca	0.001	0.001	0.000	0.002	0.003	0.002	0.000	0.002	0.000	0.000
Ni	0.030	0.022	0.029	0.025	0.030	0.033	0.027	0.031	0.027	0.028
Zn	0.005	0.006	0.006	0.008	0.010	0.009	0.007	0.009	0.006	0.014
Cr	12.210	11.445	11.084	10.935	9.722	8.864	9.089	8.382	8.163	8.013
V	0.010	0.010	0.011	0.012	0.011	0.015	0.008	0.010	0.014	0.012
Fe/Fe+Mg	0.377	0.332	0.326	0.336	0.352	0.314	0.384	0.315	0.339	0.389
Cr/Cr+Al	0.773	0.740	0.729	0.714	0.637	0.581	0.598	0.544	0.537	0.534
Fe2/Fe2 + 3	0.962	0.850	0.786	0.819	0.813	0.791	0.825	0.820	0.804	0.790
Composition of coexisiting (parental) melt										
Al_2O_3	11.8	12.4	12.7	12.9	14.5	15.0	14.8	15.4	15.3	15.3
TiO_2	0.23	0.27	0.29	0.34	0.64	0.61	0.75	0.42	0.79	0.92
mg# (max)	ND	ND	ND	0.785	0.76	ND	ND	ND	ND	ND

Amphibole

Amphiboles are commonly found as a minor interstitial phase in the shallow chromitites and more rarely in the deeper bodies. They are calcic and vary in Al-content and so range in composition from tremolite to magnesian hornblende. Al-contents vary from 1.5 to 13.0 wt% Al_2O_3, and Cr-contents from 0.08 to 2.6 wt% Cr_2O_3 (electronic supplementary material Table 2). Al and Cr correlate inversely with Si.

Olivine-orthopyroxene-spinel oxygen barometry

Only two samples contain the mineral assemblage olivine-orthopyroxene-chromite. One is the Maharra sills, the other is dunite at the Shamis locality. Application of the Ballhaus et al. (1991) oxygen geobarometer shows a small difference between the two localities. At the Maharra locality the chromitites crystallized between 1.2 and 1.6 log units above the QFM buffer and the Shamis dunites—0.1 to 0.6 log units above the QFM buffer. These data are plotted in

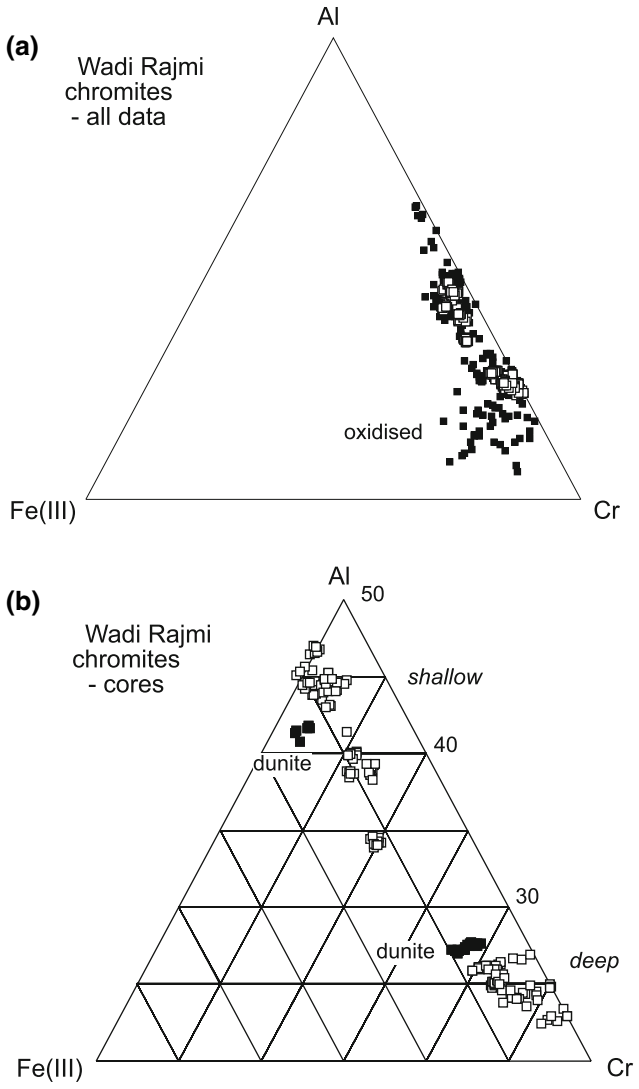

Fig. 5 **a** A ternary Al-Cr-Fe(III) plot for the Wadi Rajmi chromite rims (*black squares*) and cores (*open squares*); **b** an enlargement of the Cr–Al axis of the plot in **a** showing chromite core compositions (*white squares*) and chromites from dunites (*black squares*)

Fig. 6. The chromitite data plot in the field of chromites previously identified by Rollinson (2005) and the dunites overlap the previously defined harzburgite field. The small differences in fO_2 recorded here imply small differences in oxygen fugacity in the melts with which the chromitites and dunite-harzburgites last equilibrated.

Primary magmatic chromite compositions and melt evolution in the Wadi Rajmi chromitites

In this section textural data and chemical data are used to identify primary magmatic chromite compositions. Textural information is used to determine the order of crystallisation within individual chromitite bodies. This is

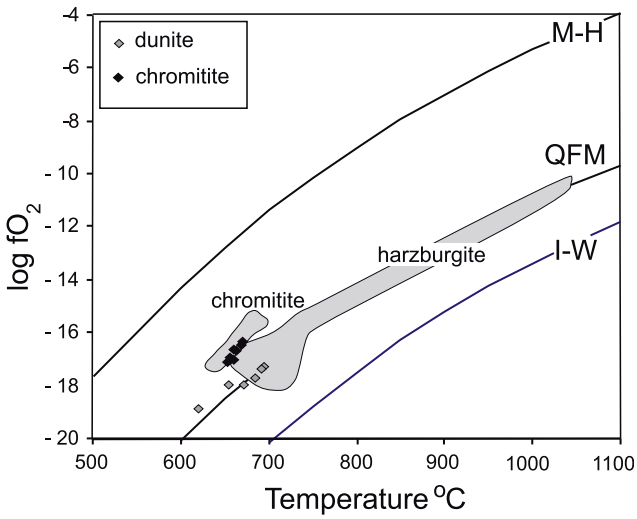

Fig. 6 Temperature-oxygen fugacity diagram showing data for Wadi Rajmi dunites and chromitites. The shaded fields of harzburgite and chromitite are from Rollinson (2005). Oxygen buffer curves are shown for magnetite–haematite (M-H), quartz–fayalite–magnetite (QFM) and iron–wustite (I–W)

principally based on the identification of cumulus and intercumulus phases and on the presence of mineral inclusions in the main phases. Detailed microprobe traverses were carried out across many of the mineral phases analysed, and these are used to assess compositional zoning within chromite, olivine and clinopyroxene. The compositional zoning is interpreted in terms of both magmatic and subsolidus exchange. However, it has earlier been noted that there has been considerable Fe–Mg exchange between coexisting mineral phases and so the primary focus here has been on the composition of mineral cores. In particular, some samples show varying core compositions in different grains within the same sample. This is interpreted as indicative of magmatic evolution. Petrographic and compositional data for the Wadi Rajmi chromitites are summarized in Table 1 and electronic supplementary material Table 1. Melt evolution as recorded in the chromites is summarized in Fig. 7. In this figure the range of compositions for a particular locality is shown as a shaded field, core compositions are shown as small squares, compositional zoning is shown by the arrows and the large squares are the likely initial composition of the chromite.

Rajmi

The Rajmi chromitites (Fig. 1) form very close to the Moho and have a gabbroic matrix suggesting a basaltic parental magma. Chromites form large subhedral grains in a matrix principally composed of clinopyroxene indicating that the chromite crystallized first and was joined by clinopyroxene. The variability in cr#, fe# and TiO_2 recorded in the chromite cores is believed to reflect the compositional

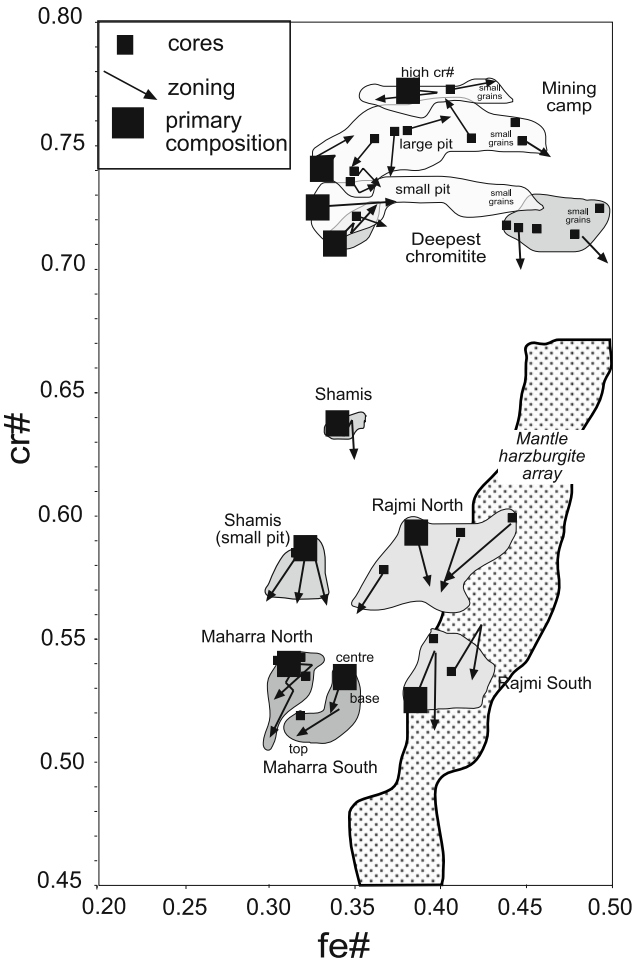

Fig. 7 The composition of chromites from the ten deposits investigated in this study showing the estimated primary chromite composition (*large squares*), other core compositions (*small squares*), all non-oxidized compositions (*grey fields*) and the pattern of zoning (*arrows*). The mantle harzburgite array is from Le Mée et al. (2004)

evolution of the melt *during* chromite crystallization. The variability in cr# shows that the Cr/Cr + Al ratio decreased (Rajmi North), or increased and then decreased (Rajmi South), during chromite crystallization (Fig. 7). The net effect of these processes was to produce a melt that evolved towards a more Fe- and Al-rich composition. The last stages of crystallisation of the melt were hydrous to produce magnesiohornblende which rims the clinopyroxene. The different cr# of Rajmi South and Rajmi North suggest that the chromitites evolved from melts that were slightly different in composition. Chromite compositions in Rajmi south overlap the field of chromites in the depleted mantle harzburgite array. This sample is a true chromitite (85% modal chromite) and not a harzburgite, and it is possible that the chromite may have formed in equilibrium with a melt similar in composition to that removed from the harzburgite. Chromite compositions from Rajmi north however are more magnesian.

Maharra

Two different chromitite 'sills' were sampled at the Maharra locality. The difference in fe# in the chromites of two sills suggests that they crystallized from slightly different batches of melt with different Fe-contents (Fig. 7). The two melts also had different Ti contents. The range of TiO_2 concentrations in chromite cores is 0.329–0.215 in the south (higher Fe) and 0.210–0.142 in the north (lower Fe). In the south the likely crystallisation sequence is chromite followed by olivine, which was subsequently replaced by orthopyroxene and clinopyroxene. Chromite core compositions suggest that as the melt crystallized it became more aluminous and more magnesian (Fig. 7). In the north chromite crystallisation was followed by orthopyroxene and clinopyroxene crystallisation. Chromite zoning indicates that the melt initially became more Fe-rich and then more magnesian. In both cases crystallisation ended with the formation a hydrous phase—interstitial amphibole. In the northern sill tremolite formed, whereas in the south a more aluminous magnesiohornblende crystallized.

Shamis

Chromite was the first phase to crystallize in the main pit at Shamis, followed by olivine. The absence of phases other than olivine in the chromitite suggests that the original melt was more magnesian and less calcic and aluminous than chromitite parental melts higher up in the succession. In the dunitic sheath surrounding the chromitites, olivine crystallisation preceded chromite. The olivine is less magnesian than that in the chromitite, but is less likely to have had its composition modified through Fe–Mg exchange with spinel. The lower cr# for chromites in the small pit at Shamis indicates that they crystallized from a more Al-rich melt than that in the main pit.

Mining camp

Samples from the Mining camp area form small irregular chromitite bands and veins and are typically discordant to structures in the mantle harzburgite (electronic supplementary material Table 1). Chromite was the first phase to crystallize, rapidly followed by olivine; the presence of olivine inclusions in chromite and chromite in olivine indicates the later cotectic crystallization of the two phases. No other primary minerals are present except for an aluminous, Ca-free amphibole, present as inclusions in chromite in one sample. The melts from the three localities are subtly different in their Cr/Al ratio (Fig. 7), but are all much more chrome-rich than melts found closer to the Moho. Individual samples show a wide range of fe#, wider than that found in the lower cr# samples. In each case large

grains have low fe# whereas smaller grains have higher fe#. This is probably the result of two processes. Some grains, particularly the small ones are Fe-enriched as a result of Fe–Mg exchange with olivine grains during cooling. On the other hand, the variable composition of the cores of larger chromite grains indicates that there was also a magmatic Fe-enrichment process taking place.

Deepest chromite pit

In the deepest chromitite pit chromite is the first mineral to crystallize in the chromitite bands subsequently joined by olivine. Two separate bands record two different chromite compositions—both with similar cr#, but with different fe#. Some chromite grains evolve towards more Fe-rich compositions suggesting that the melt evolved towards a more Fe-rich composition. The melt composition is similar to that of the 'small pit' at the mining camp locality, but shows more extreme Fe-enrichment.

Summary: two types of chromitite

The chromitites of the wadi Rajmi transect in northern Oman may be broadly subdivided into two groups on the basis of their chromite chemistry, accessory phase mineralogy, field relations and depth from the Moho (see Fig. 3, Table 3).

- Shallow chromitites form tabular, concordant bodies in the enclosing harzburgites and are frequently mantled by dunite. They have lower cr# chromites, with higher TiO_2 and are associated with clinopyroxene, orthopyroxene and magnesiohornblende. Olivine is less common. Compositional zoning in chromite grains suggests that the melts evolved towards more aluminous compositions with time.
- Deeper chromitites are smaller irregular bodies, some of which are discordant. They are also associated with a dunite sheath. They have higher-cr# chromites, with lower TiO_2, and are associated, almost exclusively with olivine. Hydrous phases are very rare and are only found as inclusions in chromite in one sample. The olivine is more magnesian and has a higher Ni-content than that in the shallower chromitites. The compositional zoning in chromite grains records melt evolution towards more Fe-rich compositions.

An estimate of the composition of the chromitite parental melts

It has been shown above that the chromitites in the Wadi Rajmi mantle section of the Oman ophiolite are of two types (Table 3). High-cr#, low-Al_2O_3, low-TiO_2 chromitites have the geochemical character of chromitites preserved in arc lavas and specifically overlap the field of chromites in boninites on a cr#–fe# diagram. These chromitites are associated with olivine and hydrous phases are absent. They are emplaced deep in the mantle sequence and their discordant nature signifies their relatively late emplacement. In contrast, lower-cr#, high-Al_2O_3, high-TiO_2 chromitites partially overlap the field of MORB lavas.

Table 3 The two types of mantle chromitite from Wadi Rajmi, Oman ophiolite

Field relationships	Shallow Tabular—mostly concordant	Deep Smaller lenses and bands—mostly discordant
Chromite cr#	0.519–0.639	0.714–0.773
Chromite fe#	0.249–0.443	0.338–0.447
Chromite Fe(III)	Slightly higher 4–5%	Lower 2–3%
Chromite TiO_2	0.136–0.600	0.150–0.242
Chromitite mineralogy	Clinopyroxene + Orthopyroxene + Hornblende + (rare olivine)	Olivine
Hydration of interstitial minerals	Wet	Dry
Dunite mineralogy	Olivine + orthopyroxene + clinopyroxene + (amphibole)	Olivine + (rare clinopyroxene)
Chromitite olivine Fo	94.4–94.8	95.1–95.9
Dunite olivine Fo	91.6	92.3 (−95.3)
NiO in olivine (wt %)	0.48–0.55	0.549–0.83
NiO in dunitic olivine	0.429	0.460
Melt evolution	Towards more Al-rich compositions	Towards more Fe-rich compositions

These chromitites have crystallized together with clino- and ortho-pyroxene ± olivine ± plagioclase. Amphibole is also present indicating that there was a small amount of water present in the melt. The chromites have a slightly higher Fe(III) content than the high-cr# chromitites. These low-cr# chromitite bodies are emplaced at shallow levels in the mantle, close to the Moho and typically are deformed into a tabular or lensoid form, concordant with structures in the mantle harzburgite, implying that they were emplaced relatively early.

In this section experimental data for chromite-melt equilibria are used to further characterize the composition of the melts from which the Wadi Rajmi mantle chromites crystallized.

Al_2O_3 and TiO_2

Kamenetsky et al. (2001) showed from chromite-melt inclusion data in volcanic rocks that there is a linear relationship between the Al_2O_3-content and the TiO_2-content of chromite and the Al_2O_3- and TiO_2-concentrations, respectively, in the melt from which the chromite crystallized. Similar observations were made by Wasylenki et al. (2003) in their compilation of 10 kb experimental data for melt-spinel Al_2O_3 equilibria during peridotite melting and by Maurel and Maurel (1982). Hence the Al_2O_3- and TiO_2-contents of the parental melts can be recovered from the chromite compositions. Using this approach, data for MORB melts in equilibrium with chromite from Kamenetsky et al. (2001) and Roeder and Reynolds (1991) were plotted for melt-Al_2O_3 vs spinel-Al_2O_3. The data were regressed in Microsoft Excel and define a power law best-fit regression line (Fig. 8a). The process was repeated for the 'arc' data set of Kamenetsky et al. (2001) and in this case a logarithmic expression was obtained. The melt-TiO_2 vs spinel-TiO_2 data were treated in the same manner and power law expressions obtained for both arc and MORB lavas (Fig. 8b). Interestingly, in both cases, the two data points from the Kamenetsky et al. (2001) data set for back-arc basin lavas plot—one close to the MORB regression line and the other close to the arc regression line.

The results of these calculations are given in Table 2 and show that chromitites from the shallow mantle with lower cr# are derived from melts with 14.5–15.4 wt% Al_2O_3 and with 0.4–0.9 wt% TiO_2. Chromitites from the deeper part of the mantle section, with higher cr# were derived from melts with 11.8–12.9 wt% Al_2O_3 and 0.23–0.34 wt% TiO_2.

mg#

Ulmer (1989) calculated from experimental studies the partitioning of Mg and Fe between olivine and basaltic melts with MgO contents between 12.6 and 20.0 wt% MgO. His results show that the partition coefficient for Fe and Mg between olivine and melt, Kd^{ol-liq}_{Fe-Mg} is a function of melt composition and pressure. From this relationship it is possible to calculate the mg# of a melt from which olivine has crystallized.

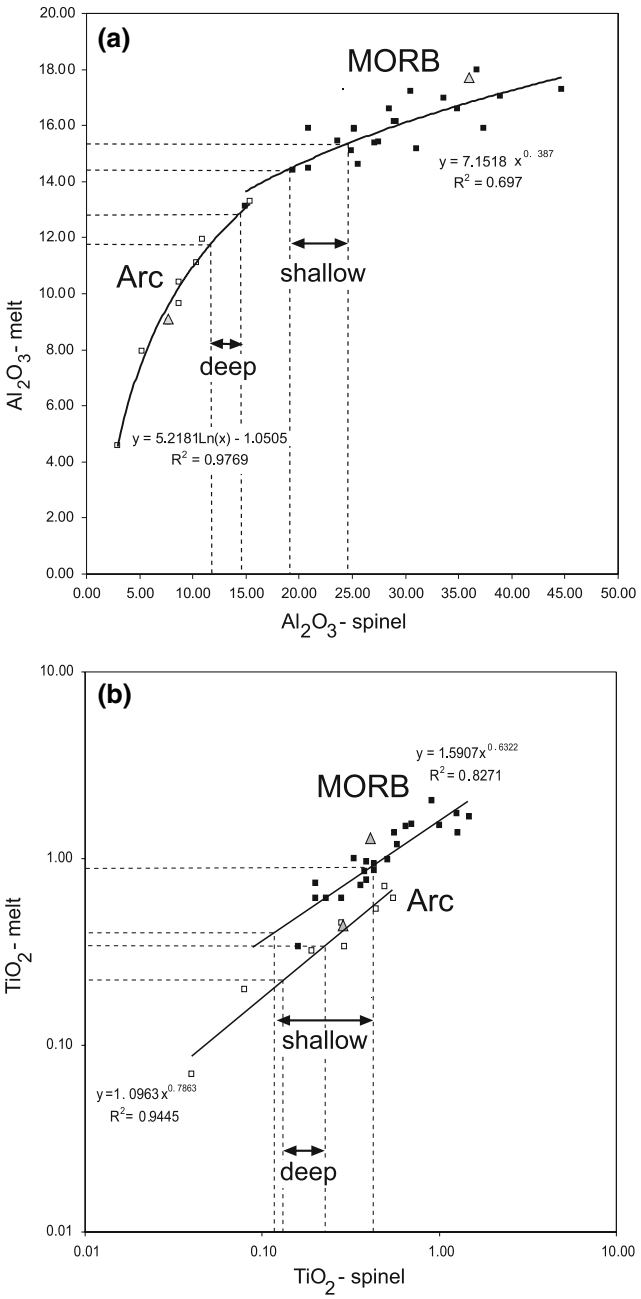

Fig. 8 Chromite-melt inclusion data for MORB (*black squares*) and arc lavas (*white squares*) from Kamenetsy et al. (2001) for Al_2O_3 (**a**) and TiO_2 (**b**). In each case the best fit regression lines are shown and the equations for the regression lines. The *dotted lines* show the range of spinel compositions from the shallow and deep Wadi Rajmi chromitites and the calculated melt compositions. The *grey triangles* are for the back-arc basin data of Kamenetsky et al. (2001)

However, it has already been shown from the results of olivine-spinel Fe–Mg exchange thermometry (Ballhaus et al. 1991) that most olivines in the Wadi Rajmi chromitites have re-equilibrated at low temperatures and so have an enhanced Fo-content, or mg#. For this reason, it has been possible to estimate melt mg# for only two melts from what are estimated to be the least-modified olivines. Both of these are from dunites where Fe–Mg exchange with other phases is likely to be minimal.

Olivine in dunite 03-13 has a core composition of $Fo_{91.2}$ which at 3 kb pressure equates to a melt mg# of 0.76. This is a maximum value, because it is possible that the mg# of the olivine is elevated above the original magmatic value. Dunite 03-13 encloses chromitite 03-12, which has a cr# of 0.64 and lies at the high end of the low-cr# chromitites. Olivine in a dunite band in sample 04-19 has a core composition of $Fo_{92.3}$ which at 3 kb pressure equates to a maximum melt mg# of 0.785. This dunite is associated with a high-cr# chromitite, cr# = 0.72.

A comparison between chromitite parental melt compositions and the composition of lavas in the Oman ophiolite

Pearce et al. (1981) showed that the lavas of the Oman ophiolite can be subdivided into two main units, which can be identified both in the field and on the basis of their geochemistry. A basal volcanic unit—termed the Geotimes Unit—is found throughout the ophiolite overlying the sheeted dyke complex. This unit has relatively high concentrations of Al_2O_3 and TiO_2 and has a close compositional affinity to mid-ocean ridge basalts (Fig. 9). Unconformably overlying the Geotimes Unit are the Lasail and Alley Units. These two units are frequently treated together, for they are compositionally similar. The Lasail and Alley Units are restricted in outcrop to the northern part of the Oman ophiolite, close to the Wadi Rajmi area, and are geochemically distinct from the Geotimes unit in having lower Al_2O_3 and TiO_2 contents (Fig. 9). They are also distinctive in having the geochemical character of arc lavas. Recently Ishikawa et al. (2002) identified boninites as lavas and dykes in the Alley Unit, further emphasising the distinctive geochemical character of the upper part of the lava succession.

To facilitate a comparison, the calculated compositions of the chromitite parent magmas are plotted on a Al_2O_3–TiO_2 diagram together with fields for the Geotimes lavas, the Lasail and Alley lavas, MORB lavas (after Godard et al. 2006) and the Oman boninites (after Ishikawa et al. 2002) (Fig. 9).

The calculated compositions of the low-cr#, shallow chromitites plot in the field of Lasail and Alley lavas, to the

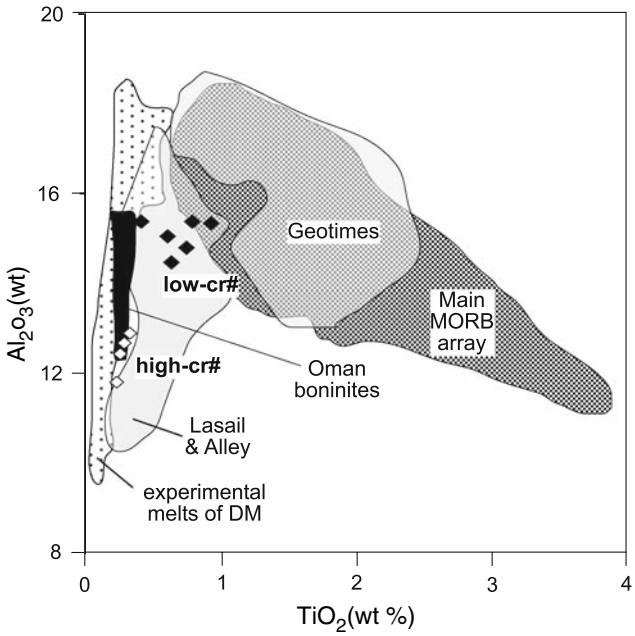

Fig. 9 TiO_2 vs. Al_2O_3 plot showing the fields of the main MORB array, the Geotimes lavas and the Lasail and Alley lavas (after Godard et al. 2006). Also shown is the field of the Oman boninites (data from Ishikawa et al. 2002) and melts of depleted mantle (DM) from Schwab and Johnston (2001) and Wasylenki et al. (2003). The calculated compositions of the parental melts to the low cr# chromitites are shown as *black diamonds* and parental melts to the high cr# chromitites as *white diamonds*

low-TiO_2 side of the Geotimes lavas and the main MORB array, indicating that the magmas parental to the low-cr# chromitites had a lower TiO_2-content than is typical of MORB. This relationship suggests that the shallow, low-cr# chromitites could be cumulates related to the Lasail and Alley lavas. The maximum mg# for the Lasail lavas is 0.74 (Godard et al. 2006) close to the value of 0.76, calculated from olivine compositions in this study. The physical proximity of the Wadi Rajmi chromitites to the relatively restricted outcrop of these upper lava units in northern Oman also supports this observation.

Schiano et al. (1997) calculated the composition of melts parental to a chromitite pod from the Maqsad area in south Oman from rehomogenized melt inclusions. The host chromites had cr# 0.52–0.58 and fe# 0.33–0.37 with matrix plagioclase and are similar in composition to the lowest of the low-cr# samples studied here. At 1,250–1,300°C the melt inclusions homogenized to the composition of olivine tholeiites and alkali basalts with mg# between 63.5 and 66.8. However, these melts have high TiO_2 and high REE concentrations and are probably represent Geotimes 'type' lavas, rather than the Lasail and Alley lavas.

The high-cr#, deeper chromitites plot well away from the MORB field, at lower Al_2O_3 and TiO_2 concentrations, close to the margin of the field of Lasail and Alley lavas

and at the lower boundary of the boninite field. This relationship is consistent with the observation made above, on the basis of the chromite cr#–fe# diagram (Fig. 2), that the high-cr# chromitites are related to boninitic lavas. Further, as noted above, the geographic proximity of the boninitic dykes and lavas of northern Oman and these chromitite pods strengthens this hypothesis. It is probable therefore that the high-cr# chromitites represent cumulates related to the Oman boninites which formed relatively deep in the mantle section.

Melt evolution in the Oman ophiolite

Experimental studies at 10 kb on the partial melting of depleted peridotites show that Ti and Al behave incompatibly and that for a given percentage of melting, both Al_2O_3 and TiO_2 concentrations are lower in melts of depleted peridotite than in melts of a MORB-source peridotite (Schwab and Johnston 2001;Wasylenki et al. 2003). Hence on a TiO_2–Al_2O_3 diagram, the field of melt compositions produced during the partial melting of depleted peridotite plots to the low TiO_2 side of the MORB field (Fig. 9). Relative to the Oman lavas plotted in Fig. 9 the field of depleted mantle melts slightly overlaps the field of Lasail and Alley lavas and overlaps the boninite field. This observation is consistent with the evidence from experimental petrology that boninites are melts of a depleted mantle source (see review by Crawford et al. 1989).

The low-cr# chromitites

The calculated melt compositions for the low-cr# chromitites lie in the field of the Lasail and Alley volcanics and have TiO_2 contents intermediate between the Geotimes (MORB) lavas and melts of the depleted mantle. Godard et al. (2006) showed that the Geotimes and Lasail–Alley volcanic units have same initial Nd and Pb isotope ratios, indicating that they were derived by the partial melting of an identical depleted-mantle, MORB-like source. However, the Lasail lavas have much lower REE concentrations and are more light-REE depleted than the Geotimes lavas, leading to the suggestion that either the Lasail lavas represent a much higher degree of partial melting (>20%) of a MORB source than do the Geotimes lavas, or that the Lasail lavas represent a low-pressure, second-stage melt of a MORB source. In addition the Lasail lavas have elevated concentrations of Pb, U and Th, identical to the pattern of trace elements found in the Oman ophiolite harzburgites. This led Godard et al. (2006) to propose that the Lasail lavas have also interacted with the shallow mantle before their eruption. The effect of this mantle–melt interaction is equivalent to the addition of a 2% melt from the mantle harzburgites.

The data presented here are consistent with a mixing model for the origin of the parental melts to the low-cr# chromitites (the Lasail lavas). Their TiO_2 contents lie between those of depleted mantle melts and the MORB array and the calculated maximum mg# for the melt of 0.76 is higher than the maximum values in primitive MORBs (mg# = 0.69–0.72, Falloon and Green 1988), and consistent with a contribution from the melt of a depleted mantle source (mg# = 0.77–0.82, Schwab and Johnston 2001). Following Godard et al. (2006) this mixing could be between a melt produced by a high degree of melting (>20%) of a MORB-source and abyssal harzburgite. This scenario is similar to that advocated by Arai and Yurimoto (1994) and Zhou et al (1994) for mantle podiform chromitite genesis and is discussed further below.

The existence of transitional lavas (Godard et al. 2006), transitional between the MORB Geotimes and the depleted Lasail lavas, may explain some of the variability in composition in the calculated melt compositions for the low-cr# chromitites (Fig. 9). For example there is some evidence that the parental melt to the Rajmi South chromitite, emplaced just below the Moho, is MORB-like. The calculated parental melt for this chromitite overlaps the main MORB array and chromite compositions in this body overlap with those of the mantle harzburgite array (Fig. 7) implying that they were in equilibrium with an MORB melt. This is the only chromitite in this study with interstitial plagioclase. Thus, in this study, the Rajmi South body is probably the closest in composition to a chromitite derived from an MORB melt.

Melts parental to the high-cr# chromitites

Crawford et al. (1989) classified boninites into low- and high-Ca varieties. The Oman boninites were defined as high-Ca and intermediate-Ca by Ishikawa et al. (2002) and here a high-Ca boninite magma is inferred as the parental melt to the high-cr# chromitites. The calculated Al_2O_3 and TiO_2 contents of the parental melt and the chromite cr# (0.714–0.773) both support this view. Chromites in high-Ca boninites have cr# (0.72–0.78) lower than that in low-Ca boninites. A maximum melt mg# of 0.785, calculated from co-existing olivine, is within the range of high-Ca boninites (0.77–0.825: Falloon and Danyushevsky 2000) but is higher than the maximum values estimated for primary MORB magmas (0.69–0.72, Falloon and Green 1988). Further support for the high-Ca boninitic character of the magmas parental to the deep, high-cr# chromitites is the observation that their calculated compositions overlap the field of high-Ca boninitic lavas in the upper pillow lava sequence of the Troodos ophiolite (Crawford et al. 1989).

There are two views on the origin of high-Ca boninites. Crawford et al. (1989), summarising the experimental

evidence, indicated that they are product of almost dry melting (<0.5 wt% H_2O in source), at low pressure (<10 kb), at temperatures between 1,250 and 1,350°C of a depleted mantle source, such as a residuum from which an MORB-melt has been extracted. Falloon and Danyushevsky (2000) on the other hand show from experimental studies that primary high-Ca boninitic melts have high MgO (19–24 wt%), and represent high temperature melts (1,400–1,500°C) fluxed with 1–2% H_2O formed at shallow mantle depths (45 km). These results are consistent with measured melt inclusion data on boninites from Tonga and from the Troodos upper pillow lavas.

Discussion

The observations presented earlier imply that there are two, perhaps three different melts contributing to the parental melts of the Oman mantle chromitites. One end-member is a melt of MORB-mantle and the others are the shallow and deep melts of depleted mantle, i.e. mantle harzburgite from which an MORB-melt has been previously extracted.

The low-cr# chromites were derived from a melt which was the product of mixing between an MORB-type melt and a melt of previously depleted mantle. These melts had chromite on the liquidus, but also crystallized clinopyroxene, amphibole and more rarely plagioclase. They are believed to be parental to the lavas of the Lasail and Alley Units. The high-cr# chromitites crystallized from a high-Ca boninitic melt in the deeper part of the mantle section after the formation of the low-cr# chromitites. These melts were generated by the re-melting of previously depleted mantle harzburgite. They fractionated in melt conduits in the mantle, leading to the formation of chromite cumulates, prior to their emplacement as the boninitic dykes and lavas of the Alley Unit.

It is likely that the source of the 'melts of depleted mantle' identified in this study are re-melts of the Oman mantle harzburgite. Depleted harzburgite compositions in the Oman ophiolite vary from 0.27 to 1.47 wt% Al_2O_3, 0.22 to 1.22 wt% CaO and 0.01 to 0.07 wt% TiO_2 (Godard et al. 2000; Gerbert-Gaillard 2002) implying variable degrees of melt extraction. REE concentrations indicate, in places, as much as 30% melt extraction (Le Mée et al. 2004). These high degrees of melt extraction could suggest that some of the Oman mantle harzburgites have experienced a second stage of melting.

Mechanisms of chromite precipitation

The findings of this study are consistent with the model for mantle chromitite genesis proposed by Arai and Yurimoto (1994) and Zhou et al. (1994; 1996). In this model a primary mantle melt reacts with mantle harzburgite on its ascent through the shallow upper mantle. The effect of the melt–rock reaction is to make the melt more siliceous, through orthopyroxene dissolution. The net effect of this is twofold. The melt composition is shifted into the field of chromite crystallisation and the host harzburgite is converted to dunite. A combination of the crystallisation of chromite from the more siliceous melt with the continued mixing of new batches of melt serves to maintain the melt composition in the field of chromite crystallisation for a protracted period of time, thus enabling the formation of chromitites. Experimental support for the model was provided by Ballhaus (1998) who found that magma mixing facilitates chromite nucleation.

The detail of the primary chromite composition diagram (Fig. 7) shows that the low-cr# chromitites have a range of cr#, supportive of the idea of the mixing of melt and host-rock, and as predicted by Zhou et al. (1996). Braun and Kelemen (2002) showed that not all melts, migrating in dunitic channels, will equilibrate with the mantle harzburgite. This provides a further explanation for the variability of melt compositions seen in this study and may be the reason why some melt compositions are believed to be close to that of MORB, as discussed earlier. Field support for the melt-reaction model comes from the abundant, dunitic, melt percolation channels in the Oman harzburgite (Kelemen et al. 1995; Braun and Kelemen 2002) and the dunitic sheaths found around chromitite pods. The melt–rock reaction mechanism was anticipated in an earlier study in which the continuum of chromite compositions on a cr#–fe# diagram and on PGE-plots also indicate a mixing origin for the Oman chromitite parental magmas (Rollinson 2005).

If the high-Ca boninitic melts, parental to the high-cr# chromitites are the product of hot, wet, deep mantle melting of depleted mantle harzburgite (Falloon and Danyushevsky 2000) they might be expected to react with mantle harzburgite at low pressure. This is borne out by the presence of the dunitic melt-reaction sheaths surrounding the high-cr# chromitites.

This study has found that in the Oman harzburgites high-percentage melts of a MORB-source mantle have reacted with depleted mantle harzburgite in the shallow mantle to produce low-cr# chromitites very close to the Moho. Later in the history of the ophiolite, second-stage melts of mantle harzburgite, parental to high-Ca boninites, precipitated high-cr# chromitites at a deeper level in the mantle. If the high-Ca boninites formed at very high temperatures at 45 km depth as proposed by Falloon and Danyushevsky (2000) then they might be expected to cool rapidly on their ascent through the mantle and leave a cumulate residue deeper in the mantle than the MORB melts.

The significance of water in the parental melts

It was shown earlier that the shallow mantle, low-cr# chromitites form in association with hydrous phases, implying a parental magma that was hydrous. The presence of hydrous phases as inclusions in chromite from mantle chromitites has been described by Lorand and Ceulneer (1989) and Schiano et al. (1997) from the Maqsad area in the south of Oman. Matveev and Ballhaus (2002) have shown experimentally the importance of water in the nucleation of chromite in basaltic systems. The origin of this water is uncertain. Zhou and Robinson (1997) imply that it is derived from a subducting slab and is indicative of a supra-subduction zone environment for mantle chromitites. Arai and Matsukage (1998) on the other hand report mantle chromites from the Hess Deep which contain hydrous mineral inclusions, indicating that the entrapment of hydrous phases in chromite can take place in magmas generated at spreading ridge. Curiously, the high-Ca boninitic melts, created through hydrous partial melting show no evidence of hydrous phases.

The geodynamic setting of the Oman mantle chromitites

The former tectonic setting of the Oman ophiolite has been the subject of debate for more than 20 years and is currently polarized into whether the Oman ophiolite formed in an ocean ridge environment or by spreading in a supra-subduction setting (Pearce et al. 1981; Boudier and Nicolas 2007; Warren et al. 2007).

Recent exponents of the ocean ridge spreading centre model for the Oman ophiolite are Le Mée et al. (2004) and Monnier et al. (2006). These authors have drawn attention to the apparent geochemical segmentation of the mantle harzburgites, which they argue indicates regions of greater and lesser melt extraction, on a scale of ca. 100 km, beneath the former spreading centre. However, as noted earlier, the Oman harzburgitic mantle may preserve a memory of more than one melt extraction event, in which case the observations of Le Mée et al. (2004) and Monnier et al. (2006) record an integrated melt extraction history, which conflates two or more different geological processes.

Other authors have come to the view that the coexistence of low-cr# 'MORB-type' chromitites with high-cr# 'boninitic-type' chromitites in the same ophiolitic mantle section indicates a marginal basin/back arc basin setting for the formation of the ophiolite (Roberts 1988; Zhou and Robinson 1997). This is a possible explanation for chromitites in the Oman ophiolite and is consistent with the lava geochemistry reported by Godard et al. (2006).

Acknowledgments This research was funded by a research grant from Sultan Qaboos University—grant number IG/SCI/ETHS/04. Stuart Kearns, University of Bristol is thanked for his generous assistance with the microprobe analysis, and Francoise Boudier and Adolphe Nicolas are thanked for introducing the author to the Oman ophiolite in the field. The comments of two anonymous reviewers helped in greatly improving this manuscript.

References

Ahmed AH, Arai S (2002) Unexpectedly high PGE chromitite from the deeper mantle section of the northern Oman ophiolite and its tectonic implications. Contrib Mineral Petrol 143:263–278

Arai S, Matsukage K (1998) Petrology of a chromitite micropod from Hess Deep, equatorial Pacific: a comparison between abyssal and alpine-type podiform chromitites. Lithos 43:1–14

Arai S, Yurimoto H (1994) Podiform chromitites of the Tari-Misaka ultramafic complex, southwestern Japan, as mantle–melt interaction products. Econ Geol 89:1279–1288

Auge T (1987) Chromite deposits in the northern Oman ophiolite: mineralogical constraints. Mineral Deposita 22:1–10

Ballhaus C (1998) Origin of podiform chromite deposits by magma mingling. Earth Planet Sci Lett 156:185–193

Ballhaus C, Berry RF, Green DH (1991) High pressure experimental calibration of the olivine-orthopyroxene-spinel oxygen geobarometer: implications for the oxidation state of the upper mantle. Contrib Mineral Petrol 107:27–40

Boudier F, Nicolas A (2007) Comment on "dating the geologic history of Oman's Semail Ophiolite: insights from U–Pb geochronology" by CJ Warren, RR Parrish, MP Searle and DJ Waters. Contrib Mineral Petrol 154:111–113

Braun MG, Kelemen PB (2002) Dunitic distribution in Oman ophiolite: implications for melt flux through porous dunite conduits. Geochem Geophys Geosyst 3:8603. doi:10.1029/2001GC000289

Ceuleneer G, Nicolas A (1985) Structures in podiform chromite from the Maqsad district (Sumail ophiolite, Oman). Mineral Deposita 20:177–185

Crawford AJ, Falloon TJ, Green DH (1989) Classification, petrogenesis and tectonic setting of boninites. In: Crawford AJ (ed) Boninites and related rocks. Unwin Hyman, London, pp 1–49

Droop GTR (1987) A general equation for estimating Fe^{3+} concentrations in ferromagnesian silicates and oxides from microprobe analysis, using stoichiometric criteria. Mineral Mag 51:431–435

Edwards SJ, Pearce JA, Freeman J (2000) New insights concerning the influence of water during the formation of podiform chromitite. Geol Soc Am Spec Pap 349:139–147

Falloon TJ, Danyushevsky LV (2000) Melting of refractory mantle at 1.5, 2.0 and 2.5 GPa under anhydrous and H_2O undersaturated conditions: implications for the petrogenesis of high-Ca boninites and the influence of subduction components on mantle melting. J Petrol 41:257–283

Falloon TJ, Green DH (1988) Anhydrous partial melting of peridotite from 8 to 35 kb and the petrogenesis of MORB. J Petrol Spec Lithosphere Issue: 379–414

Gerbert-Gaillard L (2002) Charactérisation Géochimique des péridotites de l'ophiolite d'Oman: processus magmatiques aux limites lithosphère/asthénosphère. PhD Thesis, University of Montpellier

Godard M, Jousselin D, Bodinier JL (2000) Relationships between geochemistry and structure beneath a palaeo-spreading centre: a study of the mantle section of the Oman ophiolite: an ICP-MS study. Earth Planet Sci Lett 180:133–148

Godard M, Bosch D, Einaudi F (2006) A MORB source for low-Ti magmatism in the Semail ophiolite. Chem Geol 234:58–78

Irvine TN (1965) Chromian spinel as a petrogenetic indicator. Part I. Theory. Can J Earth Sci 2:648–672

Irvine TN (1967) Chromian spinel as a petrogenetic indicator. Part II. Petrological applications. Can J Earth Sci 4:71–103

Ishikawa T, Nagaishi K, Umino S (2002) Boninitic volcanism in the Oman ophiolite: implications for thermal condition during transition from spreading ridge to arc. Geology 30:899–902

Kamenetsky VS, Crawford AJ, Meffre S (2001) Factors controlling chemistry of magmatic spinel: an empirical study of associated olivine, Cr-spinel and melt inclusions from primitive rocks. J Petrol 42:655–671

Kelemen PB, Shimizu N, Salters VJM (1995) Extraction of mid-ocean-ridge basalt from the upwelling mantle by focused flow of melt in dunite channels. Nature 375:747–753

Leblanc M, Ceulneer G (1992) Chromite crystallization in a multicellular magma flow: evidence from a chromitite dike in the Oman Ophiolite. Lithos 27:231–257

Le Mée L, Girardeau J, Monnier C (2004) Mantle segmentation along the Oman ophiolite fossil mid-ocean ridge. Nature 432:167–172

Lorand JP, Ceulneer G (1989) Silicate and base-metal sulfide inclusions in chromites from the Maqsad area (Oman ophiolite, Gulf of Oman): a model for entrapment. Lithos 22:173–190

Matveev S, Ballhaus C (2002) Role of water in the origin of podiform chromitite deposits. Earth Planet Sci Lett 203:235–243

Maurel C, Maurel P (1982) Étude expérimental de la distribution de l'aluminium entre bain silicate basique et spinelle chromifère. Implications pétrogenetiques: teneur en chrome des spinelles. Bulletin de Mineralogie 105:197–202

Monnier C, Girardeau J, Le Mée L, Polvé M (2006) Along-ridge petrological segmentation of the mantle in the Oman ophiolite. Geochem Geophys Geosyst 7:Q11008. doi:10.1029/2006GC001320

Nicolas A, Al-Azri H (1991) Chromite-rich and chromite-poor ophiolites: the Oman case. In: Peters T, Nicolas A, Coleman RG (eds) Ophiolite genesis and evolution of the oceanic lithosphere. Kluwer, Dordrecht, pp 261–274

Pearce JA, Alabaster T, Shelton AW, Searle MP (1981) The Oman ophiolite as a cretaceous arc-basin complex: evidence and implications. Phil Trans R Soc Lond A300:299–317

Roberts S (1988) Ophiolitic chromitite formation: a marginal basin phenomenon? Econ Geol 83:1034–1036

Roeder PL, Reynolds I (1991) Crystallisation of chromite and chromium solubility in basaltic melts. J Petrol 32:909–934

Rollinson HR (2005) Chromite in the mantle section of the Oman ophiolite: a new genetic model. Island Arc 14:542–550

Schiano P, Clocchiatti R, Lorand J-P, Massare D, Deloule E, Chaussidon M (1997) Primitive basaltic melts included in podiform chromites from the Oman ophiolite. Earth Planet Sci Lett 146:489–497

Schwab BE, Johnston AD (2001) Melting systematics of modally variable, compositionally intermediate peridotites and the effects of mineral fertility. J. Petrol 42:1789–1811

Ulmer P (1989) The dependence of the Fe^{2+}–Mg cation-partitioning between olivine and basaltic liquid on pressure, temperature and composition. Contrib Mineral Petrol 101:261–273

Warren CJ, Searle MP, Parrish RR, Waters DJ. (2007) Reply to comment by F. Boudier and A. Nicolas on "Dating the geologic history of Oman's Semail Ophiolite: insights from U–Pb geochronology" by CJ Warren, RR Parrish MP Searle and DJ Waters. Contrib Mineral Petrol 154:115–118

Wasylenki LE, Baker MB, Kent AJR, Stolper EM. (2003) Near-solidus melting of the shallow upper mantle: partial melting experiments on depleted peridotite. J Petrol 44:1163–1191

Zhou M-F, Robinson PT (1997) Origin and tectonic environment of podiform chromite deposits. Econ Geol 92:259–262

Zhou M-F, Robinson PT, Bai WJ (1994) Formation of podiform chromitites by melt/rock interaction in the upper mantle. Mineral Deposita 29:98–101

Zhou M-F, Robinson PT, Malpas J, Li Z (1996) Podiform chromitites in the Luobusa ophiolite (southern Tibet): implications for melt–rock interaction and chromite segregation in the upper mantle. J Petrol 37:3–21